Cerebral Cortex June 2007;17:1394-1401
doi:10.1093/cercor/bhl051
Advance Access publication August 11, 2006

Altered Neocortical Cell Density and Layer Thickness in Serotonin Transporter Knockout Mice: A Quantitation Study

C. Altamura[1], M.L. Dell'Acqua[1], R. Moessner[2], D.L. Murphy[3], K.P. Lesch[2] and Antonio M. Persico[1,4]

[1]Laboratory of Molecular Psychiatry and Neurogenetics, University "Campus Bio-Medico," Rome, Italy, [2]Department of Psychiatry and Psychotherapy, University of Wuerzburg, Wuerzburg, Germany, [3]Laboratory of Clinical Science, National Institute of Mental Health/National Institutes of Health, Bethesda, MD, USA and [4]I.R.C.C.S. "Fondazione S. Lucia," Rome, Italy

C. Altamura and M.L. Dell'Acqua contributed equally to this work

The neurotransmitter serotonin (5-HT) plays morphogenetic roles during development, and their alteration could contribute to autism pathogenesis in humans. To further characterize 5-HT's contributions to neocortical development, we assessed the thickness and neuronal cell density of various cerebral cortical areas in serotonin transporter (5-HTT) knockout (ko) mice, characterized by elevated extracellular 5-HT levels. The thickness of layer IV is decreased in 5-HTT ko mice compared with wild-type (wt) mice. The overall effect on cortical thickness, however, depends on the genetic background of the mice. Overall cortical thickness is decreased in many cortical areas of 5-HTT ko mice with a mixed c129-CD1-C57BL/6J background. Instead, 5-HTT ko mice backcrossed into the C57BL/6J background display increases in supragranular and infragranular layers, which compensate entirely for decreased layer IV thickness, resulting in unchanged or even enhanced cortical thickness. Moreover, significant increases in neuronal cell density are found in 5-HTT ko mice with a C57BL/6J background (wt:hz:ko ratio = 1.00:1.04:1.17) but not in the mixed c129-CD1-C57BL/6J 5-HTT ko animals. These results provide evidence of 5-HTT gene effects on neocortical morphology in epistatic interaction with genetic variants at other loci and may model the effect of functional 5-HTT gene variants on neocortical development in autism.

Keywords: apoptosis, cerebral cortex, optical fractionator proliferation, stereology

During embryogenesis and early postnatal development, serotonin (5-HT) regulates a wide variety of neural developmental processes, including cell proliferation, migration, differentiation, programmed cell death, cell–cell coupling, neuritic sprouting, and pruning (for review, see Di Pino and others 2004). In the central nervous system, 5-HT affects the proliferation of neural progenitor cells and the maturation of postmitotic neurons, either by binding directly to 5-HT receptors located on the progenitor cell itself or by stimulating the release of astroglial neurotrophic factors (Whitaker-Azmitia and others 1996; Azmitia 2001). Programmed cell death, another critical developmental process linking cell survival to neuronal activity and to the availability of target- or afferent-derived neurotrophic factors, is also significantly reduced in the presence of excess extracellular 5-HT (Persico and others 2003). In vitro studies indicate that morphogenetic responses to 5-HT can vary dramatically depending on the 5-HT receptor subtypes expressed by different target cells. Neurite outgrowth, for example, can be potently stimulated by 5-HT in dissociated cultures of thalamic neurons, through the activation of multiple 5-HT receptors including 5-HT_{1B}, 5-$HT_{2A/2C}$, and 5-HT_3 receptors, whereas 5-HT_{1A} receptors exert no effect in the same paradigm (Persico and others 2006) or even inhibit neuritic growth and branching in dissociated cultures of cortical neurons (Sikich and others 1990).

Altered neurodevelopment is currently recognized as the underlying neuropathological cause of several human disorders, including autism. The neuroanatomical changes ultimately responsible for altered information processing in autistic patients encompass reduced programmed cell death and/or increased cell proliferation, altered cell migration with disrupted cortical and subcortical cytoarchitectonics, abnormal cell differentiation with reduced neuronal size, and altered synaptogenesis, leading to unbalanced local versus long-distance and inhibitory versus excitatory connectivity (for review, see Levitt and others 2004; Courchesne and Pierce 2005; Pickett and London 2005; Persico and Bourgeron 2006). These alterations impinge on neurodevelopmental processes largely overlapping with those physiologically modulated by 5-HT (Di Pino and others 2004). Additional evidence of 5-HT involvement in autism pathogenesis comes from the well-established observation that a consistent subgroup of autistic patients displays elevated 5-HT blood levels (Schain and Freedman 1961; Piven and others 1991; Hérault and others 1996; Anderson and others 2000; Anderson 2002; Mulder and others 2004; Janusonis 2005). This hyperserotoninemia may be due to altered serotonin transporter (5-HTT) expression in platelets (Katsui and others 1986; Cook and others 1988; Marazziti and others 2000; Anderson and others 2002). Finally, a recent quantitative brain-imaging study has revealed increased cortical gray matter volumes in autistic patients carrying 5-HTT gene variants yielding reduced 5-HTT gene expression and slower extracellular 5-HT clearance rates (Wassink and others 2005).

These convergent findings point toward possible contributions to autism vulnerability by a dysregulation of 5-HTT gene expression, which could affect cerebral cortical growth by altering extracellular 5-HT concentrations during critical periods in neurodevelopment (see Discussion). The present study was designed to explore the potential modulatory effects of 5-HT on neocortical thickness and neuronal cell density, using a rodent model characterized by an excess of extracellular 5-HT due to 5-HTT gene inactivation (Bengel and others 1998; Mathews and others 2004).

Materials and Methods

The 5-HTT knockout (ko) mice were obtained by homologous recombination, as described previously (Bengel and others 1998). We assessed 8 animals per genotype (M:F = 4:4) from an F6 backcross into

C57BL/6J background and 7 animals per genotype (M:F = 4:3) with mixed c129-CD1-C57BL/6J background, yielding a total of 45 animals. Mice were recruited in "triplets" (i.e., wild type [wt], heterozygous [hz], and ko matched by sex and litter to control for nonspecific between-litter confounding factors) and perfused at 4–5 months of age, as described previously (Persico and others 2000, 2001). Adjacent 50-μm-thick coronal sections were processed for 1) Nissl or Giemsa staining and 2) acetylcholinesterase (AChE) histochemistry (Hedreen and others 1985), as described previously (Persico and others 2000, 2001).

The thickness of the cortex and of each cortical layer was measured on AchE-stained sections, at coronal levels corresponding to Figures 19–20, 25–27, 35–36, 43–45, and 55–58 of the atlas of Franklin and Paxinos (1997) (Fig. 1). Images were captured using the C4742 Digital CCD Camera (Hamamatsu Photonics K.K., Hamamatsu City, Japan), and linear measurements were performed using the AquaCosmos software package (version 1.20). For each layer and for the entire cortex, 3–6 measurements were taken in each cortical area and averaged to yield mean thickness measures. Measurements on the same sections were performed in parallel by C.A., M.L.D.A. and A.M.P., until an interrater reliability of ±5% was achieved for total cortical thickness and for each cortical layer measurement. This level of interrater reliability was achieved for all cortical regions, except for limbic areas (cingulate, infralimbic, and retrosplenial), where only total cortical thickness is reported due to insufficient interrater reliability of thickness measurements for single layers.

Neuronal cell densities were measured on Nissl- or Giemsa-stained sections throughout the cerebral cortex using the optical fractionator method (Gundersen and others 1988; West and others 1991), as implemented by the Stereoinvestigator imaging system (Microbrightfield Inc., Colchester, VT). This method provides precise and unbiased estimates of the total number of cells present in an organ by counting cells only in a fraction of the organ, represented by "optical dissectors." A minimum of 12 sections per animal were used, with periodicity of 2 (i.e., assessing every other section). Mice backcrossed into C57BL/6J were also assessed specifically at motor, somatosensory, and retrosplenial cortices, using all coronal sections available corresponding, respectively, to Figures 25–27 (6–8 sections), 43–45 (6–8 sections), and 53–56 (5–7 sections) of the atlas of the mouse brain of Franklin and Paxinos (1997). All stereological measurements were performed blind with respect to genotype and background. Optical dissectors were defined using an unbiased counting frame, with width (X) and height (Y) set at 30 μm, and thickness (Z) set at 10 μm, considering that following staining procedures the actual thickness of the sections was empirically found to usually correspond to 20 μm and that two 5-μm-thick guard zones were applied. These parameters were chosen following preliminary assessments and provided 1) mean (range) cell counts of 2.49 (1.35–3.12) neurons per optical dissector; 2) mean (range) number of optical dissectors examined: total cortex, 133 (124–150); motor cortex, 96 (62–120); somatosensory cortex, 79 (61–97); and retrosplenial limbic cortex, 86 (70–107); 3) actual number of cells counted: 308–373 neurons per whole cortex, 154–299 per motor cortex, 152–242 per somatosensory cortex, and 174–266 per retrosplenial limbic cortex; and 4) coefficient of variation ≤ 0.1 and usually <0.06 depending on the number of coronal sections available. Neuronal nuclei represented the counting units and were counted only as they first came into focus within each optical dissector. Neurons were distinguished from glial cells based on their size and shape. The vast majority of sections was Nissl stained; a small subset of Giemsa-stained sections were included, after mean neuronal cell counts were assessed in adjacent Nissl- and Giemsa-stained sections from the same 4 mice and found to differ only by 3.3 ± 1.5%, well within the expected sampling variance of the fractionator method.

Animals were not chosen randomly but rather according to a matched design, whereby each triplet includes 3 same-sex, same-litter adult mice carrying 5-HTT wt, hz, and ko genotypes. Therefore, cortical thickness was contrasted using a factorial analysis of variance (ANOVA) for repeated measures, as implemented by the generalized linear model for repeated measures procedure of SPSS (version 13.0), with 5-HTT genotype as within-subject factor and coronal level, cortical region, layer, and sex as between-subject factors, followed by one-way ANOVAs for repeated measures and Bonferroni's post hoc tests. One-way ANOVAs for repeated measures were also employed to analyze neuronal cell densities in these same litter– and sex–matched animals differing by 5-HTT genotype. Neuronal cell densities were obtained by dividing estimated neuronal cell counts by the volume of the cortical area outlined and assessed by the optical fractionator. Data are reported as mean ± standard error of the mean.

All experiments were performed according to protocol K3/98 approved by the Italian Ministry of Health (D.L. 116/92).

Results

The number of functionally active 5-HTT alleles exerts significant effects on cortical thickness, which vary depending on genetic background. Table 1 summarizes measurements recorded in cortical regions displaying significant genotype effects in at least 1 of the 2 genetic backgrounds (the complete data set is available in Supplementary Table 1). The most consistent finding in 5-HTT ko mice with mixed c129-CD1-C57BL/6J background is represented by a significant reduction in neocortical thickness, mostly due to a reduction in layer IV thickness, decreased overall by 10.1% and 8.9% in 5-HTT ko compared with wt and hz mice. Although this is especially evident in more frontal S1 areas, receiving somatosensory input from jaw and forelimb, more caudal S1 areas also display the same trend to a lesser extent (Table 1, left panel, and Supplementary Table 1). The thickness of layers I, II/III, and V/VI in these same regions is either unchanged or nonsignificantly reduced. A similar pattern is found in primary visual cortex, with significantly thinner layer IV, nonsignificantly reduced total cortical thickness, and no change in thickness of supragranular and infragranular layers. Also significantly reduced is the thickness of the primary motor cortex in more frontal coronal levels (Table 1, left panel), whereas no consistent trend is present in limbic areas (Supplementary Table 1).

Mice backcrossed into the C57BL/6J background also generally display a thinner layer IV, reaching statistical significance in several S1 regions (Table 1, right panel). However, no cortical region here shows significant reductions in total cortical thickness, due to the presence of thicker layers I, II/III, and/or V/VI. In contrast to mixed background mice, 5-HTT ko mice backcrossed into C57BL/6J display a trend toward increased and not decreased total cortical thickness, in several S1 areas including jaw, and more frontal forelimb and barrel fields (Table 1, right panel). Significantly increased thickness is recorded in the retrosplenial granular cortex (Table 1, right panel).

An overall factorial ANOVA for repeated measures demonstrates in mixed c129-CD1-C57BL/6J background mice a highly significant effect of "genotype" both alone and in interaction with "layer," confirming at the statistical level the notion of a genotype effect mainly affecting layer IV (Table 2; see Supplementary Table 2 for the complete summary output of the factorial ANOVA). The influence exerted by the 5-HTT genotype explains 14.3% of the variance in cortical thickness, either alone or in interaction with "layer" (Table 2). A trend favoring females over males is also present in mixed background mice, with 7.4% versus 12.6% decreases in overall cortical thickness for females and males, respectively; this trend, however, does not reach statistical significance (genotype × layer × sex, $P = 0.055$, not significant [NS]) (Supplementary Table 2). On the other hand, mice backcrossed into C57BL/6J display a highly significant effect of genotype only in interaction with cortical "region," reflecting opposite trends in ko mice between relatively thicker S1 and retrosplenial areas

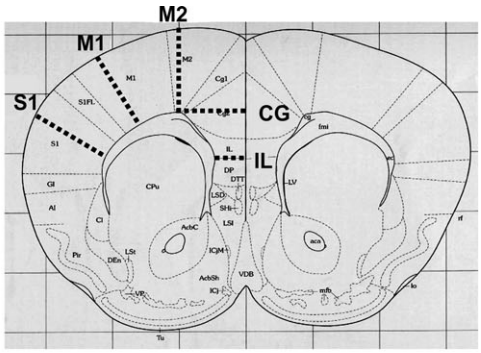

Fig. 20
I +5.14 mm
B +1.34 mm

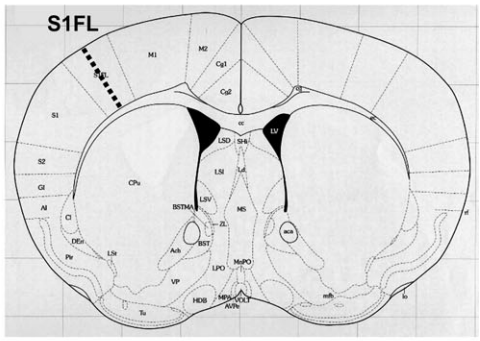

Fig. 26
I +4.42 mm
B +0.62 mm

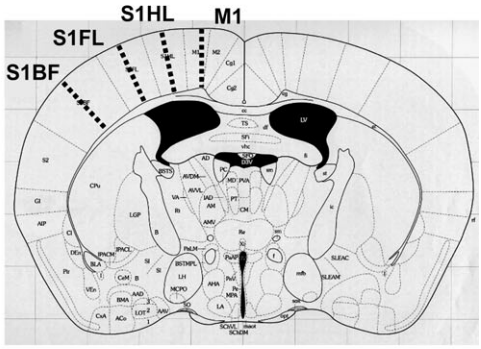

Fig. 36
I +3.22 mm
B -0.58 mm

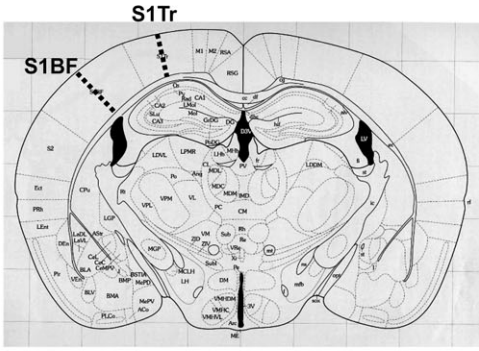

Fig. 44
I +2.22 mm
B -1.58 mm

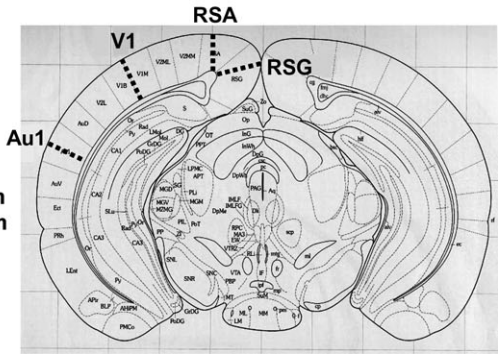

Fig. 53
I +1.10 mm
B -2.70 mm

versus unchanged or thinner cortices elsewhere. In these mice, sex effects reach statistical significance in interaction with genotype and with cortical region (Table 2). In general, ko:wt thickness ratios suggest that in most cortical areas females display either less of a decrease or more of an increase in cortical thickness compared with males, although this trend is highly region-specific (Supplementary Table 3). Overall, up to 16.6% of the variance in cortical thickness is explained by interactions between 5-HTT genotype, region, and/or sex in C57BL/6J mice (Table 2). Analyses focused exclusively on cortical areas and layers displaying statistically significant differences between 5-HTT wt, hz, and ko mice indicate that 5-HTT genotype, either alone or in interaction with other variables, can explain anywhere between 46% and 74% of the variance in thickness (Supplementary Table 4). These analyses confirm the apparent sensitivity of these cortical regions to 5-HTT allelic status.

Mean neuronal cell density measurements immediately reveal prominent background effects, with mixed c129-CD1-C57BL/6J wt mice displaying 36.2% higher mean neuronal cell density compared with C57BL/6J wt mice (Student's $t = 5.628$, 13 df, $P < 0.001$) (Fig. 2*A*). Neuronal densities measured throughout the neocortex are significantly increased in 5-HTT ko mice with C57BL/6J background (wt:hz:ko = 1.00:1.04:1.17) but not in mice with mixed c129-CD1-C57BL/6J background (Fig. 2*A*). Cortical neuronal densities are similarly enhanced in primary motor, primary somatosensory, and retrosplenial areas of 5-HTT ko mice with C57BL/6J background, although this trend achieves statistical significance only in retrosplenial limbic cortex due to interindividual variability (Fig. 2*B*). Genotype-related differences in neuronal cell density are present in both sexes and are possibly more evident in female ko mice compared with males, for the entire cortex (Fig. 2*C*) and for primary motor, primary somatosensory, and retrosplenial cortical areas assessed separately (data not shown).

Finally, 5-HTT genotypic status exerts no significant influence on body weight (mean ± SD for wt, hz, and ko = 36.5 ± 4.6, 35.8 ± 4.4, and 35.7 ± 5.1 g, respectively, $F = 0.121$, $P = 0.886$, NS) and brain weight (mean ± SD for wt, hz, and ko = 0.48 ± 0.02, 0.47 ± 0.03, and 0.45 ± 0.02 g, respectively, $F = 1.107$, $P = 0.338$, NS). The same holds true for genetic background: mice backcrossed into C57BL/6J show only a slight reduction of 3.5 g in mean body weight compared with mixed background animals regardless of 5-HTT genotype, whereas brain weights are entirely comparable.

Discussion

The present study quantitates the morphogenetic correlates of 5-HTT allelic inactivation at the neocortical level. Interest in performing this type of assessment was spurred by a recent report describing the influence of functional 5-HTT gene

Figure 1. Coronal levels and neocortical areas assessed for cortical thickness in 5-HTT wt, hz, and ko mice with either a mixed c129-CD1-C57BL/6J background or backcrossed into C57BL/6J. Figure numbers and distances from the interaural line (I) and bregma (B), expressed in millimeters, refer to the atlas of the mouse brain of Franklin and Paxinos (1997). M1, primary motor cortex; M2, secondary motor cortex; S1, primary somatosensory cortex (J, jaw; FL, forelimb; HL, hindlimb; BF, whisker barrel field; TR, trunk); CG, cingulate cortex; IL, infralimbic cortex; V1, primary visual cortex; Au1, primary auditory cortex; RS, retrosplenial cortex (A, agranular; G, granular).

Table 1
Cortical thickness in 5-HTT wt, hz, and ko mice, expressed in micrometers as mean ± standard error of the mean

	c129-CD1-C57BL/6J background, $N = 7$ (F:M = 3:4) per genotype			C57BL/6J background, $N = 8$ (F:M = 4:4) per genotype		
Figure 20	wt	hz	ko	wt	hz	ko
M1						
I	54.9 ± 10.9	55.7 ± 7.8	60.9 ± 7.6	48.3 ± 4.9	44.8 ± 4.9	54.9 ± 4.9
II–III	405.4 ± 23.7	375.4 ± 10.1	370.8 ± 27.2	416.0 ± 12.4	409.3 ± 16.5	419.6 ± 13.8
V–VI	706.7 ± 17.7	685.0 ± 7.0	670.6 ± 24.3	720.6 ± 31.2	715.4 ± 17.6	702.0 ± 26.6
Total	**1196.4 ± 25.5**	**1140.6 ± 22.7**	**1091.3 ± 20.6***	1172.1 ± 34.2	1171.3 ± 27.1	1160.5 ± 39.5
S1J						
I	76.6 ± 3.3	71.7 ± 4.2	84.7 ± 8.1	53.9 ± 7.6	42.9 ± 4.9	54.1 ± 4.3
II–III	218.6 ± 28.0	204.7 ± 23.0	175.7 ± 15.2	**234.0 ± 8.7**	**238.6 ± 14.2**	**274.9 ± 13.1***
IV	**244.9 ± 14.0**	**231.7 ± 16.7**	**196.6 ± 7.4***	257.0 ± 14.4	251.9 ± 11.9	237.4 ± 11.2
V–VI	726.4 ± 34.6	743.6 ± 25.2	710.4 ± 20.6	743.8 ± 13.3	739.6 ± 21.4	753.3 ± 23.2
Total	**1287.4 ± 36.9**	**1269.3 ± 45.1**	**1203.1 ± 35.8***	1297.8 ± 27.2	1285.1 ± 30.4	1343.4 ± 31.6
Figure 26						
S1FL						
I	68.7 ± 8.1	69.6 ± 4.3	66.0 ± 4.2	44.0 ± 2.9	40.9 ± 4.1	52.1 ± 3.7
II–III	231.6 ± 17.9	215.0 ± 12.9	211.7 ± 17.8	228.4 ± 8.5	242.3 ± 8.9	253.4 ± 13.9
IV	**217.6 ± 5.8**	**221.4 ± 11.6**	**190.0 ± 6.8***	218.6 ± 11.5	232.4 ± 15.5	222.8 ± 8.5
V–VI	563.4 ± 16.0	538.6 ± 13.1	532.3 ± 18.3	**646.4 ± 18.3**	**633.6 ± 8.7**	**671.1 ± 24.3***
Total	1104.1 ± 26.8	1083.4 ± 26.9	1003.4 ± 22.1	1133.6 ± 27.6	1158.4 ± 24.2	1201.4 ± 38.8
Figure 36						
S1FL						
I	62.7 ± 8.2	63.0 ± 4.8	65.6 ± 5.9	39.6 ± 3.0	46.4 ± 2.9	44.1 ± 3.6
II–III	205.6 ± 14.0	204.6 ± 7.7	204.4 ± 14.9	215.4 ± 13.1	219.5 ± 15.0	231.8 ± 12.9
IV	182.0 ± 8.0	169.4 ± 7.3	169.4 ± 9.2	**225.9 ± 12.2**	**208.0 ± 6.8**	**193.5 ± 6.2***
V–VI	539.7 ± 17.7	535.1 ± 17.3	536.4 ± 17.4	587.5 ± 14.7	582.0 ± 13.5	580.4 ± 13.7
Total	1006.7 ± 25.6	1005.0 ± 26.7	982.0 ± 21.7	1082.9 ± 26.3	1063.8 ± 26.8	1056.8 ± 21.5
S1HL						
I	65.6 ± 7.1	66.7 ± 4.4	61.6 ± 4.6	38.3 ± 2.2	46.0 ± 4.6	44.5 ± 3.4
II–III	191.7 ± 11.4	194.7 ± 12.9	203.0 ± 11.4	209.0 ± 12.8	217.6 ± 10.7	226.1 ± 8.9
IV	162.9 ± 7.3	164.1 ± 9.6	151.9 ± 5.0	**212.0 ± 11.1**	**186.4 ± 7.0**	**179.4 ± 8.7***
V–VI	544.3 ± 12.7	501.9 ± 18.2	533.4 ± 17.8	597.1 ± 12.4	593.1 ± 15.3	567.3 ± 14.3
Total	994.3 ± 15.8	959.0 ± 27.9	957.4 ± 31.8	1068.1 ± 23.7	1050.5 ± 26.2	1018.1 ± 18.9
S1BF						
I	69.3 ± 7.1	69.0 ± 8.1	69.9 ± 7.4	**37.3 ± 2.7**	**41.4 ± 2.8**	**47.3 ± 2.8****
II–III	228.3 ± 15.6	230.4 ± 11.7	223.6 ± 10.3	233.9 ± 10.5	239.8 ± 9.4	257.1 ± 12.3
IV	235.4 ± 12.6	225.9 ± 15.8	215.3 ± 9.4	**259.4 ± 7.4**	**246.2 ± 8.8**	**235.6 ± 5.3***
V–VI	507.9 ± 11.1	493.1 ± 13.2	496.4 ± 10.7	595.0 ± 15.2	600.4 ± 15.6	606.3 ± 20.8
Total	**1080.0 ± 23.1**	**1046.4 ± 15.8**	**1014.6 ± 24.0***	1132.4 ± 22.9	1138.3 ± 20.9	1169.0 ± 29.7
Figure 53						
V1						
I	47.0 ± 5.5	49.3 ± 3.1	53.9 ± 4.0	37.2 ± 1.8	40.7 ± 1.8	41.0 ± 2.6
II–III	158.7 ± 12.2	156.0 ± 13.8	149.6 ± 13.1	166.2 ± 9.4	159.7 ± 9.2	161.5 ± 10.5
IV	**138.6 ± 4.2**	**144.6 ± 8.6**	**116.6 ± 7.6****	172.0 ± 10.1	174.2 ± 13.9	172.7 ± 6.0
V–VI	263.6 ± 9.1	254.7 ± 10.3	259.1 ± 5.5	275.8 ± 11.0	284.8 ± 4.4	275.0 ± 6.1
Total	611.4 ± 14.7	612.6 ± 19.6	584.7 ± 17.9	656.7 ± 18.2	666.3 ± 21.9	652.0 ± 11.9
Aud1						
I	71.0 ± 11.2	64.3 ± 5.8	60.9 ± 5.8	40.6 ± 3.2	42.9 ± 2.4	46.8 ± 3.5
II–III	147.7 ± 5.5	167.1 ± 7.9	167.0 ± 27.9	**178.4 ± 11.5**	**187.9 ± 12.1**	**150.9 ± 8.5***
IV	146.9 ± 12.8	150.1 ± 6.5	138.6 ± 9.3	166.4 ± 6.8	176.4 ± 4.2	180.0 ± 6.1
V–VI	360.7 ± 28.1	343.6 ± 15.8	308.3 ± 24.4	412.3 ± 15.5	395.0 ± 15.0	407.6 ± 12.6
Total	753.1 ± 43.9	736.1 ± 23.2	718.1 ± 29.4	807.5 ± 24.3	818.1 ± 23.1	781.0 ± 18.0
RS (granular)	894.8 ± 38.8	885.8 ± 70.7	826.8 ± 52.2	**833.3 ± 37.8**	**915.9 ± 66.8**	**1037.0 ± 67.0***

Note: M1, primary motor cortex; S1, primary somatosensory cortex (J, jaw; FL, forelimb; HL, hindlimb; BF, whisker barrel field; TR, trunk); V1, primary visual cortex; Aud1, primary auditory cortex; RS, retrosplenial cortex. wt vs. ko *$P < 0.05$, **$P < 0.01$.

variants on cortical gray matter volume in autistic patients (Wassink and others 2005). Our results demonstrate that the 5-HTT gene can affect neocortical thickness and neuronal cell density in epistatic interaction with other loci, whose functional variants are dyshomogeneously distributed among different mouse strains.

Both parameters assessed in this study, that is, cortical thickness and neuronal cell density, have been measured in a consistent number of sex- and litter-matched mice differing only in genotype and background. The frequent intra- and interrater reliability checks performed throughout the study for both parameters, the consistency of measurements by raters blind to genotype and background, the steps taken to minimize random sampling error rates in stereological studies, the lack of nonspecific genotype-related differences in body and brain weight, and the congruency of our results with previously published literature on 5-HT trophic effects at the neocortical level (for review, see Luo and others 2003; Di Pino and others 2004) all enhance confidence in the reliability of these findings.

The morphological characteristic most directly linked to 5-HTT null status is represented by a thinner layer IV (Table 1). Thalamocortical endings transiently express the 5-HTT and $5HT_{1B}$ receptors during early postnatal life in rodents (Bennett-Clarke and others 1993; Lebrand and others 1996). Reuptake through the 5-HTT is primarily responsible for removing 5-HT from the extracellular space and for limiting its action on 5-HT membrane receptors. Not surprisingly, in vivo microdialysis experiments performed in adult 5-HTT ko mice have

Table 2

Factorial ANOVA for repeated measures performed using dependent variable = cortical thickness in micrometer, within-subject factor = 5-HTT genotype (wt/hz/ko), between-subject factors = coronal level, region, layer, sex; expressed using the Wilks λ and related *F* statistics (degrees of freedom)

Factors and interactions	Wilks λ	*F* (df)	*P* value	% Variance explained
c129-CD1-C57BL/6J				
Genotype	0.908	15.556 (2,306)	<0.001	9.2
Genotype × layer	0.901	4.089 (8,612)	<0.001	5.1
C57BL/6J				
Genotype × region	0.845	3.407 (18,698)	<0.001	8.1
Genotype × region × sex	0.887	2.400 (18,698)	<0.01	5.8
Genotype × sex	0.973	4.929 (2,349)	<0.01	2.7

Note. The strength of the effects is expressed as percentage of variance in cortical thickness explained by the factor or interaction, as estimated by partial η^2. Only statistically significant factors and interactions are listed.

demonstrated 6- and 10-fold increases in striatal and frontal cortical extracellular 5-HT, respectively (Mathews and others 2004). Convergent evidence from 5-HTT ko mice and from MAO-A ko mice, another animal model characterized by excessive extracellular 5-HT levels, indicates that the altered segregation and arborization patterns of thalamocortical terminals due to reduced extracellular 5-HT clearance and $5HT_{1B}$ receptor overstimulation can affect the thickness of layer IV (Cases and others 1995; Holschneider and others 2001; Persico and others 2001; Salichon and others 2001; Luo and others 2003). The radial spread of thalamocortical arbors in MAO-A ko mice is indeed decreased, with an impressive 50% reduction in terminal branches exclusively found in layer IV (Rebsam and others 2002). Although parallels between different species must be drawn with caution, it is interesting that healthy humans carrying the "low-expression" 5-HTTLPR (i.e., serotonin transporter gene-linked polymorphic region) "short" (s) allele associated with slower extracellular 5-HT clearance (see below) show significantly smaller gray matter volumes in several neocortical regions (Canli and others 2005).

The compensatory increase in thickness of supragranular and infragranular layers recorded only in 5-HTT ko mice backcrossed into C57BL/6J likely represents a more complex response, potentially involving both neuronal cells and neuropil. The enhanced neuronal cell densities described for the first time in this study (Fig. 2) could stem from reduced prenatal/early postnatal apoptotic cell death (Persico and others 2003). Interestingly, neuronal cell densities here display an increasing frontocaudal gradient (Fig. 2*B*), which parallels the gradient of antiapoptotic 5-HT effects previously demonstrated in these same backcrossed animals (Persico and others 2003). Additional contributions to increased cellularity could also come from 5-HT–enhanced proliferation of neuronal progenitors, by analogy with 5-HT proliferative effects recorded in a variety of in vitro and in vivo systems (for review, see Whitaker-Azmitia and others 1996; Fanburg and Lee 1997; Azmitia 2001; Di Pino and others 2004). In either case, the lack of 5-HTT genotype effects on cellularity in mixed c129-CD1-C57BL/6J mice is likely due to a "ceiling" effect, given the substantially higher neuronal density already present in mixed background wt mice compared with C57BL/6J wt mice (Fig. 2*A*). In addition to enhanced cellularity, the increased thickness of supragranular and infragranular layers is also likely to reflect an overgrowth of neuropil, especially in light of the impressive 5-HT effects on neurite length and branching recorded in organotypic or dissociated cultures of neocortical and thalamic neurons (Chubakov and others 1986; Lieske and others 1999; Lotto and others 1999; Persico and others 2006). Both activity-dependent and activity-independent mechanisms could underlie 5-HT trophic effects on neurites, as suggested on the one hand by their sensitivity to tetrodotoxin in vitro (Lotto and others 1999) and on the other hand by direct serotoninergic modulation of trophic factors, guidance cues, and migration stop signals as relevant as brain-derived neurotrophic factor (BDNF), Netrin-1, and Reelin (Vaidya and others 1997; Janusonis and others 2004; Bonnin and others 2005). It is not surprising that the vast array of polymorphic genes encoding these and other molecules likely mediating 5-HT trophic effects on supragranular and infragranular layers yield significant neuroanatomical differences in 5-HTT ko mice with different genetic backgrounds.

The morphological features of backcrossed 5-HTT ko mice described in this study display interesting parallels with several neuroanatomical abnormalities found in autistic brains (for review, see Pickett and London 2005), including increased neuronal packing densities in structures such as hippocampus, amygdala, and enthorinal cortex (Kemper and Bauman 1998); increased numbers of neurons in the cerebral cortex (Bailey and others 1998); and smaller cortical minicolumns compatible with increased short-range association fibers (i.e., local neurite elongation and sprouting and/or reduced pruning) (Casanova and others 2002; Casanova 2004). Moreover, autistic children between 2 and 16 years of age display faster-than-normal head growth rates (Piven and others 1996; Courchesne and others 2001), leading to overt macrocephaly in approximately 20% of the patients (Woodhouse and others 1996; Lainhart and others 1997; Stevenson and others 1997; Fombonne and others 1999; Miles and others 2000; Dementieva and others 2005). This brain overgrowth, encompassing both cortical gray and white matter volumes (Piven and others 1996; Bailey and others 1998; Courchesne and others 2001), could receive contributions from altered 5-HT neurotransmission, as strongly suggested by the positive association between cortical gray matter volume and the number of 5-HTTLPR s alleles recently described in autistic patients (Wassink and others 2005). The 5-HTTLPR is a polymorphic repetitive element present in the promoter region of the 5-HTT gene in humans (Lesch and others 1996); compared with the "long" (l) allele, the s allele has been shown both in vitro and in vivo to yield approximately half as much 5-HTT gene expression, resulting in slower 5-HT clearance kinetics and higher extracellular 5-HT concentrations (for review, see Murphy and others 2001). The association between increased cortical gray matter volumes and alleles yielding reduced 5-HT transport activity seemingly supports extracellular 5-HT roles in stimulating the abnormal head growth rates found in macrocephalic autistic patients. Within this framework, the apparent discrepancy between 5-HTT allelic effects on neocortical volumes of autistic patients (Wassink and others 2005) and normal individuals (Canli and others 2005) could at least partly stem from the dramatically different temporal courses of their 5-HT synthesis capacity during early childhood: normal children seemingly display 5-HT synthesis capacity above 200% of adult values until the age of 5 years, then declining to adult values; in autistic children, 5-HT synthesis capacity increases gradually over the same age span, reaching a plateau at mean levels 50% higher than adult normal values (Chugani and others 1999). Finally, the neuroanatomical differences between 5-HTT ko mice with different genetic

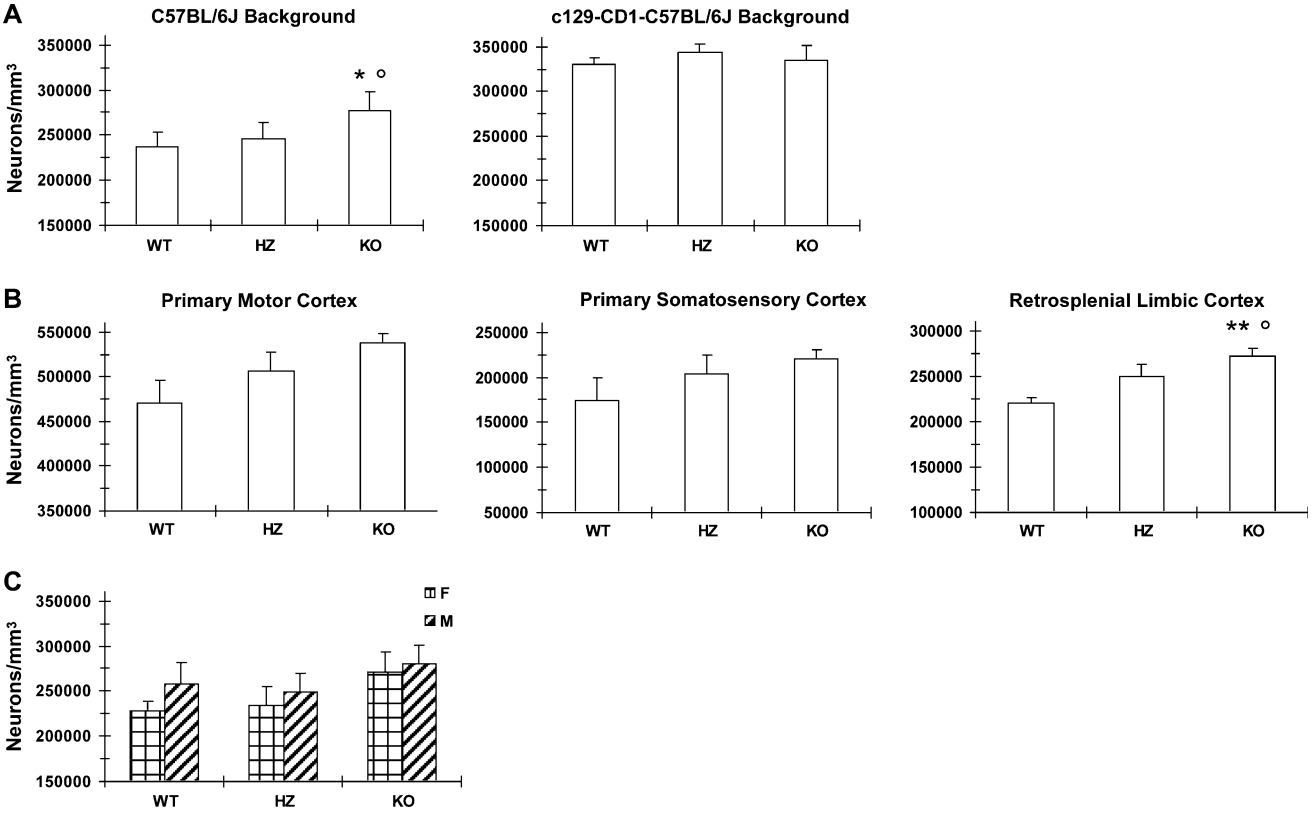

Figure 2. Neuronal density histogram obtained from (*A*) the entire cerebral cortex of 8 mice (M:F = 4:4) per genotype from an F6 backcross into C57BL/6J and from 7 mice (M:F = 4:3) per genotype with mixed c129-CD1-C57BL/6J background and from (*B*) the primary motor, primary somatosensory, and retrosplenial cortices assessed at coronal sections corresponding to Figures 25–27, 43–45, and 53–56 of the atlas of the mouse brain of Franklin and Paxinos (1997), only in 7 mice per genotype backcrossed into C57BL/6J. Data are expressed as mean ± standard error of the mean. ko versus wt: $*P < 0.05$, $**P < 0.01$. ko versus hz, $^{\circ}P < 0.05$.

backgrounds nicely parallel the significant interindividual heterogeneity in neuroanatomical, biochemical, and clinical parameters present among autistic patients. Therefore, although caution must be exercised when drawing parallels between different species, developmental stages, and health conditions, and although our results do not at all imply that 5-HTT ko mice represent altogether an animal model of autistic disorder, the specific neuroanatomical feature of increased cortical gray matter volume in autistic patients carrying the s allele is indeed mimicked by the increased neocortical thickness and neuronal cell density we describe in 5-HTT ko mice backcrossed into C57BL/6J.

An alternative mechanistic hypothesis would envision 5-HTT molecules directly exerting trophic effects not by regulating extracellular 5-HT levels but instead by inducing, for example, the formation of intracellular oxidative metabolites, as already shown in vascular smooth muscle, Burkitt lymphoma, and cerebellar granule cells (Zilkha-Falb and others 1997; Lee and others 1999; Serafeim and others 2002). These effects are blocked by selective serotonin reuptake inhibitors, whereas they are insensitive to 5-HT receptor agonists and antagonists acting on 5-HT membrane receptors. In this scenario, 5-HTT gene inactivation would be predicted to yield not a gain but rather a loss of trophic function. Currently available evidence does not appear to support this view. In fact, not only are 5-HT effects on layer IV mediated by extracellular 5-HT and $5HT_{1B}$ receptors, as previously discussed, but also increased gray matter volumes in autism are associated with the 5-HTT low-expression alleles and not the opposite (Wassink and others 2005). Moreover, elevated 5-HT blood levels may reflect enhanced 5-HTT gene expression, yielding increased densities of functionally active 5-HTT molecules on platelet membranes (Katsui and others 1986; Marazziti and others 2000). Conversely, the platelets of 5-HTT ko mice contain negligible amounts of 5-HT as they cannot uptake the 5-HT present in the plasma through the action of the 5-HTT (Chen and others 2001). Contrary to the hypothesis of direct 5-HTT–mediated trophic roles, we find no correlation at all between 5-HT blood levels and cranial circumference in a clinical sample, including well over 200 autistic patients (R Sacco and AM Persico, unpublished observation). Therefore, the neuroanatomical correlates of 5-HTT gene inactivation described in this study appear at this stage to stem from elevated extracellular 5-HT levels. However, more research will be necessary to fully understand 5-HTT roles in intracellular oxidative metabolism because, for example, 5-HTT ko mice surprisingly display enhanced and not reduced hippocampal DNA oxidation (Moessner and others 2002).

The neuroanatomical abnormalities found in this animal model further underscore the potential relevance of 5-HTT gene variants in normal and pathological human neurodevelopment. Considering the antiapoptotic effects of 5-HT (Persico and others 2003) and the sensitivity of neuronal morphogenesis in vitro to as little as picomolar or 1 nM 5-HT concentrations (Lotto and others 1999; Persico and others 2006), it is reasonable to speculate that the neurobiological processes underlying increased gray matter volumes in autistic children with genetically reduced 5-HT uptake may at least partly overlap with

those involved in the increased cortical thickness and neuronal cell density displayed here by backcrossed mice following 5-HTT gene inactivation. The opposite structural correlates of 5-HTT gene variants recorded in autistic and normal individuals suggest that the genetic and neurobiological underpinnings of autism are likely to boost 5-HT trophic effects, in epistatic interaction with polymorphic gene variants present at several loci including the 5-HTT gene.

Supplementary Material

Supplementary material can be found at: http://www.cercor.oxfordjournals.org/.

Notes

The authors thank Dietmar Bengel, Flavio Keller, and Ramona Marino for their collaboration. This work was funded through the European Community (BMH4-CT96-0730, LSHM-CT-2003-503474), Telethon-Italy (E.1215 and GGP02019), the Deutsche Forschungsgemeinschaft (SFB 581), and a grant from CaRiSal. *Conflict of Interest*: None declared.

Address correspondence to Antonio M. Persico, MD, Laboratory of Molecular Psychiatry and Neurogenetics, University "Campus Bio-Medico," Via Longoni 83, I-00155 Rome, Italy. Email: a.persico@unicampus.it.

References

Anderson GM. 2002. Genetics of childhood disorders: XLV. Autism, part 4: serotonin in autism. J Am Acad Child Adolesc Psychiatry 41:1513–1516.

Anderson GM, Gutknecht L, Cohen DJ, Brailly-Tabard S, Cohen JH, Ferrari P, Roubertoux PL, Tordjman S. 2002. Serotonin transporter promoter variants in autism: functional effects and relationship to platelet hyperserotonemia. Mol Psychiatry 7:831–836.

Azmitia EC. 2001. Modern views of an ancient chemical: serotonin effects on cell proliferation, maturation, and apoptosis. Brain Res Bull 56:413–424.

Bailey A, Luthert P, Dean A, Harding B, Janota I, Montgomery M, Rutter M, Lantos P. 1998. A clinicopathological study of autism. Brain 121:889–905.

Bengel D, Murphy DL, Andrews AM, Wichems CH, Feltner D, Heils A, Moessner R, Westphal H, Lesch KP. 1998. Altered brain serotonin homeostasis and locomotor insensitivity to 3,4-methylenedioxymethamphetamine ("Ecstasy") in serotonin transporter-deficient mice. Mol Pharmacol 53:649–655.

Bennett-Clarke CA, Leslie MJ, Chiaia NL, Rhoades RW. 1993. Serotonin 1B receptors in the developing somatosensory and visual cortices are located on thalamocortical axons. Proc Natl Acad Sci USA 90:153–157.

Bonnin A, Torii M, Levitt P. 2005. Serotonin modulates the response of embryonic thalamocortical axons to guidance cues. Program No. 481.15, 2005 Abstract Viewer/Itinerary Planner. Washington, DC: Society for Neuroscience [online].

Canli T, Omura K, Haas BW, Fallgatter A, Constable RT, Lesch KP. 2005. Beyond affect: a role for genetic variation of the serotonin transporter in neural activation during a cognitive attention task. Proc Natl Acad Sci USA 102:12224–12229.

Casanova MF. 2004. White matter volume increase and minicolumns in autism. Ann Neurol 56:453.

Casanova MF, Buxhoeveden DP, Switala AE, Roy E. 2002. Neuronal density and architecture (gray level index) in the brains of autistic patients. J Child Neurol 17:515–521.

Cases O, Seif I, Grimsby J, Gaspar P, Chen K, Pournin S, Muller U, Aguet M, Babinet C, Shih JC, and others. 1995. Aggressive behavior and altered amounts of brain serotonin and norepinephrine in mice lacking MAOA. Science 268:1763–1766.

Chen JJ, Li Z, Pan H, Murphy DL, Tamir H, Koepsell H, Gershon MD. 2001. Maintenance of serotonin in the intestinal mucosa and ganglia of mice that lack the high-affinity serotonin transporter: abnormal intestinal motility and the expression of cation transporters. J Neurosci 21:6348–6361.

Chubakov AR, Gromova EA, Konovalov GV, Sarkisova EF, Chumasov EI. 1986. The effects of serotonin on the morpho-functional development of rat cerebral neocortex in tissue culture. Brain Res 369:285–297.

Chugani DC, Muzik O, Behen M, Rothermel R, Janisse JJ, Lee J, Chugani HT. 1999. Developmental changes in brain serotonin synthesis capacity in autistic and nonautistic children. Ann Neurol 45:287–295.

Cook EH Jr, Leventhal BL, Freedman DX. 1988. Free serotonin in plasma: autistic children and their first-degree relatives. Biol Psychiatry 24:488–491.

Courchesne E, Karns CM, Davis HR, Ziccardi R, Carper RA, Tigue ZD, Chisum HJ, Moses P, Pierce K, Lord C, and others. 2001. Unusual brain growth patterns in early life in patients with autistic disorder: an MRI study. Neurology 57:245–254.

Courchesne E, Pierce K. 2005. Why the frontal cortex in autism might be talking only to itself: local over-connectivity but long-distance disconnection. Curr Opin Neurobiol 15:225–230.

Dementieva YA, Vance DD, Donnelly SL, Elston LA, Wolpert CM, Ravan SA, DeLong GR, Abramson RK, Wright HH, Cuccaro ML. 2005. Accelerated head growth in early development of individuals with autism. Pediatr Neurol 32:102–108.

Di Pino G, Moessner R, Lesch KP, Lauder JM, Persico AM. 2004. Roles for serotonin in neurodevelopment: more than just neural transmission. Curr Neuropharmacol 2:403–418.

Fanburg BL, Lee SL. 1997. A new role for an old molecule: serotonin as a mitogen. Am J Physiol 272:L795–L806.

Fombonne E, Rogé B, Claverie J, Courty S, Frémolle J. 1999. Microcephaly and macrocephaly in autism. J Autism Dev Disord 29:113–119.

Franklin KBJ, Paxinos G. 1997. The mouse brain in stereotaxic coordinates. San Diego, CA: Academic Press.

Gundersen HJ, Bagger P, Bendtsen TF, Evans SM, Korbo L, Marcussen N, Moller A, Nielsen K, Nyengaard JR, Pakkenberg B, and others. 1988. The new stereological tools: dissector, fractionator, nucleator and point sampled intercepts and their use in pathological research and diagnosis. Acta Pathol Microbiol Immunol Scand 96:857–881.

Hedreen JC, Bacon SJ, Price DL. 1985. A modified histochemical technique to visualize acetylcholinesterase-containing axons. J Histochem Cytochem 33:134–140.

Hérault J, Petit E, Martineau J, Cherpi C, Perrot A, Barthélémy C, Lelord G, Muh JP. 1996. Serotonin and autism: biochemical and molecular biology features. Psychiatry Res 65:33–43.

Holschneider DP, Chen K, Seif I, Shih JC. 2001. Biochemical, behavioral, physiologic, and neurodevelopmental changes in mice deficient in monoamine oxidase A or B. Brain Res Bull 56:453–462.

Janusonis S. 2005. Statistical distribution of blood serotonin as a predictor of early autistic brain abnormalities. Theor Biol Med Model 2:27.

Janusonis S, Gluncic V, Rakic P. 2004. Early serotonergic projections to Cajal-Retzius cells: relevance for cortical development. J Neurosci 24:1652–1659.

Katsui T, Okuda M, Usuda S, Koizumi T. 1986. Kinetics of ^{3}H-serotonin uptake by platelets in infantile autism and developmental language disorder (including five pairs of twins). J Autism Dev Disord 16:69–76.

Kemper TL, Bauman M. 1998. Neuropathology of infantile autism. J Neuropathol Exp Neurol 57:645–652.

Lainhart JE, Piven J, Wzorek M, Landa R, Santangelo SL, Coon H, Folstein SE. 1997. Macrocephaly in children and adults with autism. J Am Acad Child Adolesc Psychiatry 36:282–290.

Lebrand C, Cases O, Adelbrecht C, Doye A, Alvarez C, El Mestikawy S, Seif I, Gaspar P. 1996. Transient uptake and storage of serotonin in developing thalamic neurons. Neuron 17:823–835.

Lee SL, Wang WW, Finaly GA, Fanburg FL. 1999. Serotonin stimulates mitogen-activated protein kinase activity through the formation of superoxide anions. Am J Physiol 277:L282–L291.

Lesch KP, Bengel D, Heils A, Sabol SZ, Greenberg BD, Petri S, Benjamin J, Muller CR, Hamer DH, Murphy DL. 1996. Association of anxiety-related traits with a polymorphism in the serotonin transporter gene regulatory region. Science 274:1527–1531.

Levitt P, Eagleson KL, Powell EM. 2004. Regulation of neocortical interneuron development and the implications for neurodevelopmental disorders. Trends Neurosci 27:400–406.
Lieske V, Bennett-Clarke CA, Rhoades RW. 1999. Effects of serotonin on neurite outgrowth from thalamic neurons in vitro. Neuroscience 90:967–974.
Lotto B, Upton L, Price DJ, Gaspar P. 1999. Serotonin receptor activation enhances neurite outgrowth of thalamic neurones in rodents. Neurosci Lett 269:87–90.
Luo X, Persico AM, Lauder JM. 2003. Serotoninergic regulation of somatosensory cortical development: lessons from genetic mouse models. Dev Neurosci 25:173–183.
Marazziti D, Muratori F, Cesari A, Masala I, Baroni S, Giannaccini G, Dell'Osso L, Cosenza A, Pfanner P, Cassano GB. 2000. Increased density of the platelet serotonin transporter in autism. Pharmacopsychiatry 33:165–168.
Mathews TA, Fedele DE, Coppelli FM, Avila AM, Murphy DL, Andrews AM. 2004. Gene dose-dependent alterations in extraneuronal serotonin but not dopamine in mice with reduced serotonin transporter expression. J Neurosci Methods 140:169–181.
Miles JH, Hadden LL, Takahashi TN, Hillman RE. 2000. Head circumference is an independent clinical finding associated with autism. Am J Med Genet 95:339–350.
Moessner R, Dringen R, Persico AM, Janetzky B, Okladnova O, Albert D, Gotz M, Benninghoff J, Schmitt A, Gerlach M, and others. 2002. Increased hippocampal DNA oxidation in serotonin transporter deficient mice. J Neural Trans 109:557–565.
Mulder EJ, Anderson GM, Kema IP, de Bildt A, van Lang ND, den Boer JA, Minderaa RB. 2004. Platelet serotonin levels in pervasive developmental disorders and mental retardation: diagnostic group differences, within-group distribution, and behavioral correlates. J Am Acad Child Adolesc Psychiatry 43:491–499.
Murphy DL, Li Q, Engel S, Wichems C, Andrews A, Lesch KP, Uhl G. 2001. Genetic perspectives on the serotonin transporter. Brain Res Bull 56:487–494.
Persico AM, Altamura C, Calia E, Puglisi-Allegra S, Ventura R, Lucchese F, Keller F. 2000. Serotonin depletion and barrel cortex development: impact of growth impairment vs 5-HT effects on thalamocortical endings. Cereb Cortex 10:181–191.
Persico AM, Baldi A, Dell'Acqua ML, Moessner R, Murphy DL, Lesch KP, Keller F. 2003. Reduced programmed cell death in brains of serotonin transporter knockout mice. Neuroreport 14:341–344.
Persico AM, Bourgeron T. 2006. Searching for ways out of the autism maze: genetic, epigenetic, and environmental clues. Trends Neurosci 29:349–358.
Persico AM, Di Pino G, Levitt P. 2006. Multiple receptors mediate the trophic effects of serotonin on ventroposterior thalamic neurons in vitro. Brain Res 1095:17–25.
Persico AM, Mengual E, Moessner R, Revay RS, Sora I, Arellano J, DeFelipe J, Giménez-Amaya JM, Conciatori M, Marino R, and others. 2001. Barrel pattern formation requires serotonin uptake by thalamocortical afferents, and not vesicular monoamine release. J Neurosci 21:6862–6873.
Pickett J, London E. 2005. The neuropathology of autism: a review. J Neuropathol Exp Neurol 64:925–935.
Piven J, Arndt S, Bailey J, Andreasen N. 1996. Regional brain enlargement in autism: a magnetic resonance imaging study. J Am Acad Child Adolesc Psychiatry 35:530–536.
Piven J, Tsai G, Nehme E, Coyle JT, Chase GA, Folstein SE. 1991. Platelet serotonin, a possible marker for familial autism. J Autism Dev Disord 21:51–59.
Rebsam A, Seif I, Gaspar P. 2002. Refinement of thalamocortical arbors and emergence of barrel domains in the primary somatosensory cortex: a study of normal and monoamine oxidase A knock-out mice. J Neurosci 22:8541–8552.
Salichon N, Gaspar P, Upton AL, Picaud S, Hanoun N, Hamon M, De Maeyer E, Murphy DL, Mossner R, Lesch KP, and others. 2001. Excessive activation of serotonin (5-HT) 1B receptors disrupts the formation of sensory maps in monoamine oxidase A and 5-HT transporter knock-out mice. J Neurosci 21:884–896.
Schain RJ, Freedman DX. 1961. Studies on 5-hydroxyindole metabolism in autistic and other mentally retarded children. J Pediatr 58:315–320.
Serafeim A, Grafton G, Chamba A, Gregory CD, Blakely RD, Bowery NG, Barnes NM, Gordon J. 2002. 5-Hydroxytryptamine drives apoptosis in biopsylike Burkitt lymphoma cells: reversal by selective serotonin reuptake inhibitors. Blood 99:2545–2553.
Sikich L, Hickok JM, Todd RD. 1990. $5HT_{1A}$ receptors control neurite branching during development. Dev Brain Res 56:269–274.
Stevenson RE, Schroer RJ, Skinner C, Fender D, Simensen RJ. 1997. Autism and macrocephaly. Lancet 349:1744–1745.
Vaidya VA, Marek GJ, Aghajanian GK, Duman RS. 1997. $5\text{-}HT_{2A}$ receptor-mediated regulation of brain-derived neurotrophic factor mRNA in rat hippocampus and the neocortex. J Neurosci. 17:205–214.
Wassink TH, Cody H, Mosconi M, Epping E, Piven J. 2005. Cortical and amygdala overgrowth in autism associated with 5-HTTLPR. *Neuropsychopharmacol* 30:S116.
West MJ, Slomianka L, Gundersen HJ. 1991. Unbiased stereological estimation of the total number of neurons in the subdivisions of the rat hippocampus using the optical fractionator. Anat Rec 231:482–497.
Whitaker-Azmitia PM, Druse M, Walker P, Lauder JM. 1996. Serotonin as a developmental signal. Behav Brain Res 73:19–29.
Woodhouse W, Bailey A, Rutter M, Bolton P, Baird G, Le Couteur A. 1996. Head circumference in autism and other pervasive developmental disorders. J Child Psychol Psychiat 37:665–671.
Zilkha-Falb R, Ziv I, Nardi N, Offen D, Melamed E, Barzilai A. 1997. Monoamine-induced apoptotic neuronal cell death. Cell Mol Neurobiol 17:101–118.